THE CHEMICAL RECORD

Personal Accounts by Leading Experts

2020
20/01

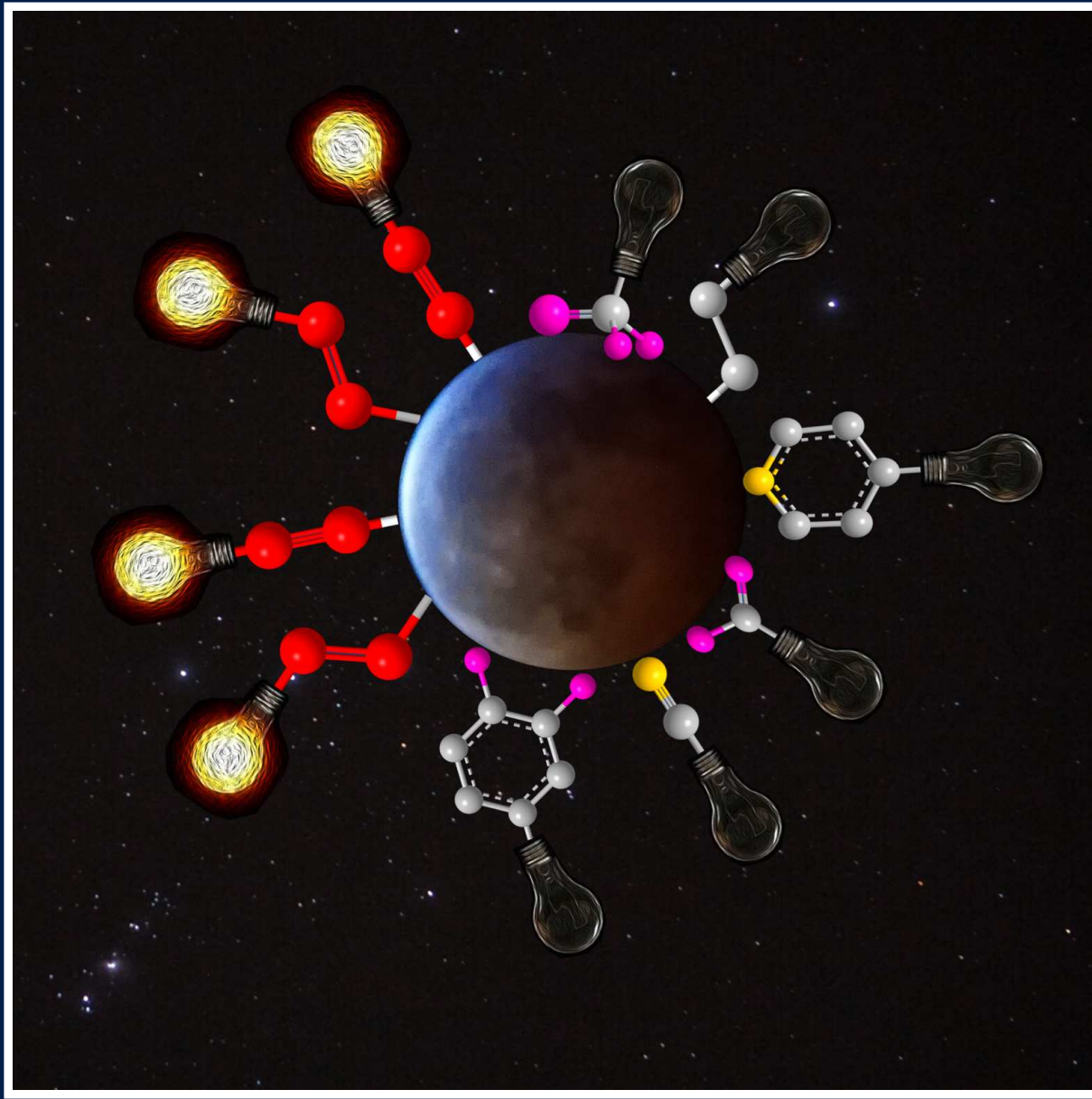

A Journal of
the Chemical
Society of Japan

WILEY-VCH

Personal Account

DOI: 10.1002/tcr.201900010

THE CHEMICAL RECORD

Structural Engineering of Semiconductor Nanoparticles by Conjugated Interfacial Bonds

Yi Peng, Qiming Liu, and Shaowei Chen*[a]

Abstract: Surface functionalization of semiconductor nanoparticles plays a significant role in the manipulation of the nanoparticle physicochemical properties and diverse applications. Conventional points of anchor involve mercapto, carboxyl and phenol moieties, forming largely nonconjugated interfacial linkages. In this personal account, we summarize recent progress in surface functionalization of semiconductor nanoparticles with olefin and acetylene derivatives, where the formation of conjugated interfacial bonds leads to ready manipulation of the nanoparticle optical and electronic properties, by using Si and TiO_2 nanoparticles as the illustrating examples. Finally, a perspective is included where the promises and challenges of structural engineering of semiconductor nanoparicles are highlighted.

Keywords: semiconductor nanoparticle, surface anchor, conjugated linkage, charge transfer, silicon, titanium dioxide

1. Introduction

Semiconductor nanoparticles represent a unique class of functional nanomaterials that have found diverse applications, such as catalysis, optoelectronics, bioimaging, and biodiagnosis.[1–3] These include a wide range of materials, such as pure elements of silicon and germanium, and compound semiconductors of transition-metal oxide, chalcogenide, nitride, and carbide.[4–5] Analogous to their metallic counterparts, semiconductor nanoparticles are generally stabilized with select organic capping ligands involving a range of interfacial linkages.[6–7] Such surface passivation enhances the dispersibility of the nanoparticles in controlled media and can lead to ready manipulation of the materials properties, such as hydrophobicity/hydrophilicity, surface charge (zeta potential), optical characteristics, catalytic performance, and so on. Thus, the selection of surface passivation ligands is important for both fundamental research and practical applications.[8–12]

A diverse range of surface capping ligands have been used, ranging from small molecules to metal complexes and to polymeric matrices, involving physical adsorption or chemical bonding.[6,13–16] In physical adsorption, the driving force entails van de Waals interaction, electrostatic interaction, and/or hydrogen bonding between the semiconductors and capping ligands.[17–21] By contrast, chemical bonding is far more stable, which can be achieved with a variey of anchoring groups.

It should be noted that in these earlier studies, the semiconductor nanoparticle-ligand interactions involve mostly non-conjugated linkages, which significantly limits the electronic coupling between the nanoparticle core and functional moieties of the capping ligands. Thus, a large amount of energy is needed to induce charge transfer across the interface.[22–23]

One immediate question arises. Will it be possible to functionalize semiconductor nanoparticles with conjugated interfacial bonds? Prior research has shown that when (transition) metal nanoparticles are capped with conjugated metal-ligand bonds, effective intraparticle charge transfer occurs between nanoparticle-bound functional moieties, lead-

[a] *Y. Peng,[+] Q. Liu,[+] Prof. Dr. S. Chen*
Department of Chemistry and Biochemistry, University of California, 1156 High Street, Santa Cruz, CA 95064, USA
E-mail: shaowei@ucsc.edu
[+] *These two authors contributed equally to the work.*

ing to the emergence of new optical and electronic properties that are analogous to those of their dimeric counterparts.[24] Recently, it has been shown that such interfacial chemistry can be extended to various semiconductor nanoparticles, such as silicene and titanium dioxide nanoparticles.

In this personal account, we summarize recent progress in organic functionalization of semiconductor nanoparticles with conjugated interfacial bonds. This is achieved by using olefin and acetylene derivatives as the capping ligands. In the first section, we focus on elemental semiconductors like silicon, and compare the materials properties within the context of three interfacial linkages, Si–CH_2–CH_2–, Si–CH=CH–, and Si–C≡C–, by taking advantage of the unique surface activity of silicon-hydride (Si–H). In the second section, we extend the study to metal oxide nanoparticles, such as TiO_2, where the formation of Ti–O–C≡C– interfacial linkage is found to facilitate charge delocalization across the core-ligand interface. This has substantial implications in the nanoparticle photoluminescence properties and photocatalytic activity. Results from these studies offer a unique chemical platform for interfacial engineering of semiconductor nanoparticle materials by enriching the tool box of nanoparticle surface functionalization. Motivated by these breakthroughs, a prospective is included highlighting the promises and challenges in future research.

2. Elemental Semiconductors

Silicon is a remarkable semiconductor and has been widely used in electronics, optics, and photovoltaics.[25–29] For nano-sized silicon, it shows novel, tunable optical and electronic properties, where surface functionalization plays a critical role. Early studies[30–31] have shown that porous silicon can be readily functionalized with alkenes/alkynes through ethylaluminum dichloride ($EtAlCl_2$) mediated hydrosilylation. Similar surface chemistry has also been employed to stabilize and functionalize silicon nanoparticles by the formation of Si–C, Si–C=,[31–39] and Si–C≡[40] interfacial bonds, in addition to other covalent linkages, such as Si–O,[41] Si–N,[42–43] and Si-halide.[44]

Experimentally, to covalently functionalize silicon (including Si nanoparticles, silicene quantum dots, etc), the silicon surface is in general activated by chemical etching to produce silicon-hydride moieties (Si–H). When the hydrogenated Si surface is exposed to olefin or acetylene derivatives, surface hydrosilylation occurs under relatively mild conditions, such as UV photoirradiation, heat, microwave or (organo)metallic catalysts, leading to the formation of Si–CH_2–CH_2– or Si-CH=CH– interfacial linkages.[32,34,45–46] The former involves saturated interfacial bonds, whereas the latter exhibits conjugated characters.

Such surface modification is schematically depicted in Figure 1a. For instance, for alkenyl-capped silicon nanoparticles prepared with acetylene derivatives (e.g., 1-ethynyl-3-

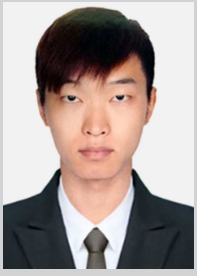

Yi Peng received his B.S. degree in Chemistry in 2014 from Beihang University, Beijing, China, and then went on to the University of California at Santa Cruz (UCSC) to pursue a Ph.D. degree in Chemistry under the supervision of Professor Shaowei Chen. His research interests include metal/semiconductor nanoparticle surface functionalization, nanoparticle charge-transfer dynamics, and single atom catalysts for electrochemical energy conversion and storage.

Qiming Liu received his B.S. degree in Materials Science and Engineering in 2018 from Central South University, Hunan, China. He then joined Professor Shaowei Chen's lab as a graduate student to pursue a Ph.D. degree. His research interests concentrate on single-atom electrocatalysts and surface functionalization of nanoparticles.

Shaowei Chen received his B.S. degree in Chemistry from the University of Science and Technology of China in 1991, and his M.S. and Ph.D. degrees from Cornell University in 1993 and 1996, respectively. Following a postdoctoral appointment at the University of North Carolina at Chapel Hill, he started his independent career in Southern Illinois University in 1998. In 2004, he moved to UCSC. He is currently a professor of chemistry and the faculty director of the UCSC COSMOS program. His research interests are primarily focused on high-performance catalysts for electrochemical energy conversion and storage, impacts of metal–ligand interfacial bonding interactions on nanoparticle charge-transfer dynamics, Janus nanoparticles by interfacial engineering, and antimicrobial activity of functional nanomaterials.

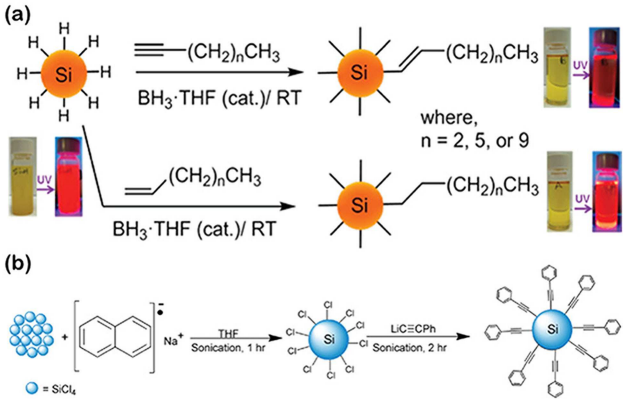

Figure 1. (a) Borane-catalyzed functionalization of hydride-terminated silicon nanoparticles with olefin/acetylene derivatives to yield an alkyl/alkenyl surface capping layer. Reprinted with permission from ref.[32] © 2014 American Chemical Society. (b) Synthesis of phenylacetylene-capped silicon nanoparticles. Reprinted with permission from ref.[40] © 2014 The Royal Society of Chemistry.

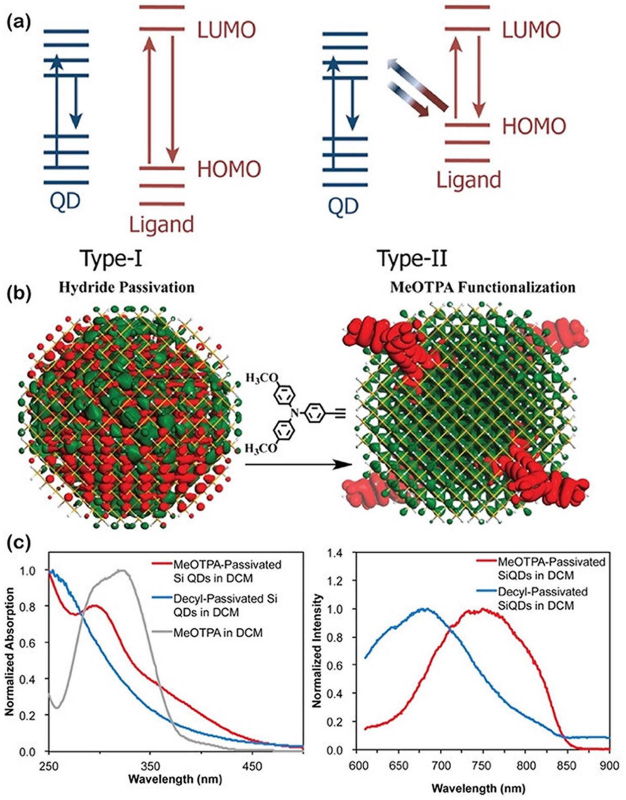

Figure 2. (a) Electronic transition in (left) Type-I and (right) Type-II molecular orbital energy level aligned organically functionalized silicon nanoparticles. (b) HOMO (red) and LUMO (green) isosurfaces from TD-DFT analysis of a 3.1 nm $Si_{849}H_{344}$ nanoparticle capped (left) by hydride only and (right) by hydride and four MeOTPA ligands. Isosurfaces are for a fixed, absolute value of electron orbitals, 0.009 $Å^{-3/2}$. (c) (left) Absorption and (right) photoluminescence spectra of MeOTPA and decyl-passivated silicon nanoparticles in dichloromethane. Reprinted with permission from ref.[50] © 2015 American Chemical Society.

flurobenzene, 3-ethynylthiophene, phenylacetylene),[32] the conjugated characteristics of the interfacial linkage is found to lead to diminishment and a slight red shift of the photoluminescence emission (Figure 1a), as compared to the alkyl-capped counterparts, due to enhanced interfacial conductivity and the formation of a deep trap in the nanoparticle.[34] These observations suggest a ready control of the nanoparticle electronic property (bandgap) simply by the disparity of surface functionalization.

Notably, for alkyl-passivated Si nanoparticles, the core bandgap is also found to diminish, albeit slightly, as compared to that of the hydrogenated precursor. This has been demonsted in *ab initio* calculations by Reboredo and Galli.[47] Interestingly, they observed an apparent shift of the relative energy (with respect to the vacuum) of the LUMO and the HOMO with the carbon chain length, which led to a decrease of the ionization potentials and electron affinities of the silicon cores, in comparison with the hydride-terminated counterparts. In addition, calculations based on time-dependent density functional theory (TD-DFT)[48] also showed that in excitation spectral measurements within the energy window of zero to three times the bandgap, the absorption of silicon nanoparticles capped with methyl/hexyl groups could increase by up to 45 %.

In another study,[49] Li et al. carried out DFT studies to examine the differences between alkyl- and alkenyl-modified silicon nanoparticles. The alkyl-modified nanoparticles were found to exhibit a type-I energy structure, which showed only limited charge transfer across the interface; whereas the alkenyl-modified counterparts displayed a type-II energy configuration owning to interfacial conjugation that facilitated interfacial charge transport (Figure 2a). In complementary experimental studies, they anchored 4-ethynyl-N,N-bis(4-methoxyphenyl)aniline (MeOTPA) onto Si nanoparticles (Figure 2b) and measured the optical absorption and photoluminescence properties.[50] From Figure 2c, one can see that MeOTPA functionalization led to the formation of a type-II energy structure of the nanoparticles, and hence enhanced absorption and red-shift (by 70 nm) of the photoluminescence emission, as compared to the decyl-capped ones. These were ascribed to direct relaxation of the charge-transfer excited state, in good agreement with results from DFT calculations.

Recently, Veinot and coworkers[33] prepared Si nanoparticles covalently grafted with ploy(3-hexylthiophene) (P3HT) to form a donor (P3HT)-acceptor (Si nanoparticles) interface. Because of the formation of conjugated Si-thiophene interfacial bonds, the resulting Si@P3HT hybrids exhibited effective quenching of the photoluminescence, a behavior totally different from that of a physical mixture of silicon

nanoparticles and P3HT. Scanning tunneling spectroscopic measurements indeed showed the formation of an apparent in-gap state near the valence band (VB) edge that was attributed to the HOMO level of P3HT.

Modification of Si surfaces with acetylene derivatives can also be achieved by nucleophilic substitution of halide-terminated surfaces with organolithium reagents.[40] As shown in Figure 1b, Ashby et al.[40] prepared phenylacetylene-capped Si nanoparticles using lithium phenylacetylide. They found that the Si–C≡C– conjugated linkage further improved the conductivity of the Si nanoparticles and the thermoelectric activity, as compared to other silicon-based materials. This was accounted for by a higher Seebeck coefficient due to a higher concentration of charge carriers introduced by conjugated capping ligands. Nevertheless, studies have been scarce focusing on the charge transfer property of Si–C=C– modified Si nanoparticles.

Recently we carried out a series of studies whereby transition-metal nanoparticles were functionalized with conjugated metal-ligand bonds and observed apparent intraparticle charge delocalization between the particle-bound functional moieties.[24] One unique phenomenon is nanoparticle-mediated intervalence charge transfer (IVCT), as manifested by spectroscopic and electrochemical measurements using ferrocene as the molecular probe. For semiconductor nanoparticles, because of the apparent bandgap and reduced electrical conductivity of the nanoparticle cores, IVCT is generally impeded. Yet under appropriate stimuli, the nanoparticles may become electrically conductive by, for instance, photoirradiation and thermal excitation, such that intraparticle charge transfer can occur. This has indeed been demonstrated recently.[51–52] In one study,[51] silicon nanoparticles, with a diameter of 2.96 ± 0.46 nm and bandgap of ca. 2.6 eV, were functionalized with vinylferrocene (VFc) and ethynylferrocene (EFc) by surface hydrosilylation under UV photoirradiation (Figure 1a). The formation of Si–CH_2–CH_2–Fc and Si–CH=CH–Fc interfacial bonds was confirmed by FTIR measurements, and XPS studies suggested a full monolayer coverage on the nanoparticle surface, which stabilized the nanoparticles against aggregation, as manifested in TEM measurements. Interestingly, square-wave voltammetric (SWVs) measurements of the SiEFc nanoparticles showed only a single pair of voltammetric peaks in the dark (blue curves, Figure 3a) that were ascribed to the redox reaction ($Fc \leftrightarrow Fc^+ + e^-$) of nanoparticle-bounded ferrocene moieties, indicating no apparent IVCT. Yet, under UV photoirradiation (black curve), two pairs of voltammetric peaks could be deconvoluted, at the formal potentials of -0.032 and $+0.093$ V (red and green curves), consistent with results observed in earlier studies of metal nanoparticle-based IVCT.[24,53–55] This was interpreted by photoenhanced conductivity of the Si nanoparticle cores that facilitated intraparticle charge transfer. In

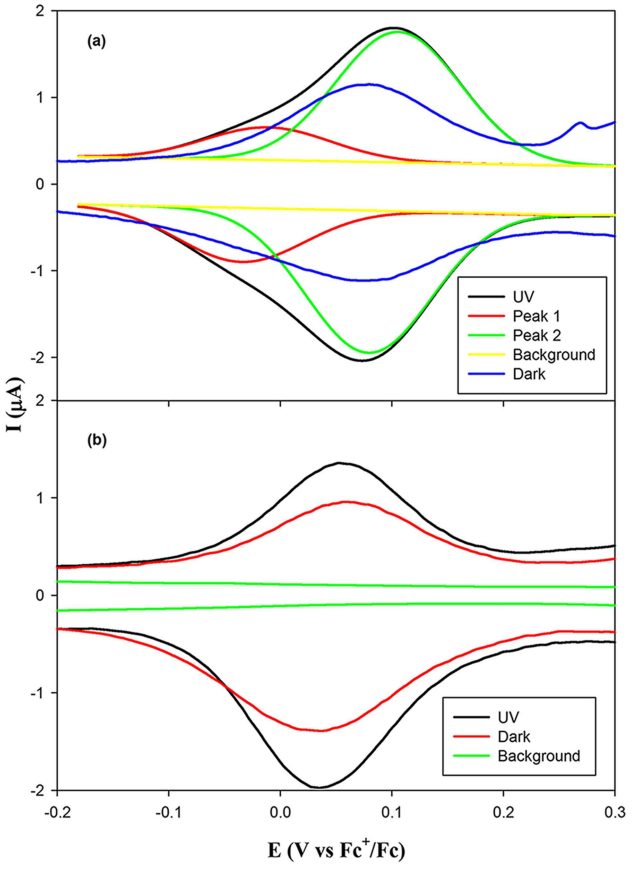

Figure 3. SWVs of (a) SiEFc and (b) SiVFc nanoparticles in 0.1 M TBAP in DMF in the dark and under UV photoirradiation (365 nm, 6 mW). SWVs collected with the blank supporting electrolyte are also included. Nanoparticle concentration: 10 mg mL^{-1}; increment of potential: 2 mV; amplitude: 25 mV; frequency: 15 Hz. Red and green curves in (a) are the deconvolution fits of the voltammograms acquired under UV photoirradiation. Reprinted with permission from ref.[51] © 2016 WILEY-VCH Verlag GmbH & Co. KGaA, Weinheim.

sharp contrast, for SiVFc where the ferrocene moieties were bound onto the nanoparticle surface by saturated interfacial linkages, voltammetric measurements yielded only a single pair of peaks both in the dark and under UV photoirradiation (Figure 3b), indicating that the saturated linkages effectively impeded electronic communication between the ferrocene moieties on the nanoparticle surface and they behaved individually. Similar behaviors have also been observed with silicene quantum dots.[52]

Germanium is another semiconductor in the same group. A range of synthetic strategies have been reported in the literature for the preparation of germanium nanoparticles, and amine derivatives represent the most commonly used ligands for the surface functionalization of the nanoparticles.[56–58] The limitation of nanoparticle surface chemistry is likely due to the instability of the nanoparticles under ambient conditions.

Similar to the silicon counterparts, alkyl/alkenyl-capped germanium nanoparticles can also be made by hydrogermylation of alkenes/alkynes on hydrogenated germanium nanoparticles,[59] a unique property that can be exploited, for instance, for the preparation of germanium nanoparticles with a hydrophobic or hydrophilic surface. Further research is desired to expand the tool box for germanium nanoparticle functionalization, in particular, involving conjugated interfacial bonds, such that more complicated manipulation of the nanoparticle optical and electronic properties can be achieved.

3. Metal Oxides

Metal oxides represent a large family of semiconductor materials, and carboxylic acids have been widely used as surface capping ligands for metal oxide nanoparticles,[60–75] where several structural models have been proposed to account for the interfacial bonding interactions between –COOH and metal oxide surface, such as monodentate ester, bidentate chelating, bidentate bridging, H-bonded, etc. Yet, the chemical nature of the interfacial linkage has remained under active debate.[76] Although electron transfer can occur across the carboxylic-oxide interface, the electronic coupling between the nanoparticles and surface ligands remains relatively weak, limiting the efficiency of interfacial charge transfer.[60–62,68]

In recent years, a variety of anchor groups, such as boronic acid, hydroxamic acid, and phosphonic acid, have also been used to replace carboxylic acid/carboxylate ligands for metal-oxide nanoparticle surface functionalization, where the structural stability is enhanced due to the increasingly robust chemical bonding.[77–86] For example, metal oxide nanoparticle surface can be functionalized with phosphonic acid derivatives, forming (−M–O–P–) bonds[87–88] or with boronic acid which can condense with the hydroxy goups on metal oxide surface to form (−M–O–B−) bonds.[77]

Other anchoring groups have also been used for metal oxide nanoparticles. For instance, isocynate (–NCO) ligands can adsorb onto metal oxide surfaces by additive reaction with surface hydroxy groups forming (–NHCOOM–) bonds.[89–90] Pyridine moieties anchor onto semiconductor nanoparticles surface by strong coordination between the lone-pair electrons on pyridinic N sites and Lewis acid sites of metals, leading to efficient electron-withdrawing injection.[91–93] Tetrazole has several N as coordination sites to form –M–N– bonding.[94] Acetylacetonate can chelate a metal ion at an oxygen defect of a metal oxide surface.[95] Phenolic hydroxy derivatives, such as catechol, dopamine, calixarene, sulfocalixarene, and fullerol, have also been used for metal oxide/cholcogenide surface functionalization, where condensation reaction with surface-bound hydroxy groups leads to the formation of –M–O–R bonds.[96–105]

It should be noted that in these earlier studies, the ligand-oxide interfacial bonds are mostly nonconjugated in nature. In a recent study,[106] we demonstrated that metal oxide nanoparticles could also be functionalized with conjugated interfacial linkages by using acetylene derivatives as the capping ligands. The resulting nanoparticles exhibited markedly different optical and electronic properties, as compared to those capped with conventional ligands like carboxylic acids. Experimentally, TiO_2 nanoparticles were used as the illustrating example, because of its wide applications in diverse areas. The nanoparticles were prepared and capped with acetylene by a two-phase synthetic approach.[106–107] Experimental studies, in conjunction with DFT calculations, were carried out to investigate the chemical and electronic structure of the interface. Firstly, DFT calculations suggested that energetically the most stable interfacial linkage was Ti–O–C≡C– which resulted in the shortening of the C–O bond and elongation of the C≡C bond, as compared to their pristine counterparts, due to partial charge transfer from the π-electrons in C≡C to TiO_2. Figure 4a depicts the density of state (DOS) plots of a TiO_2 slab with and without surface ligands. Clearly, the DOS profiles of TiO_2 slabs functionalized by acetate or ethyl ligands are similar to that of a pristine TiO_2 slab with a band gap of 2.2 eV. However, for the TiO_2 slab functionalized with acetylenyl ligands, a new state emerged between the valence

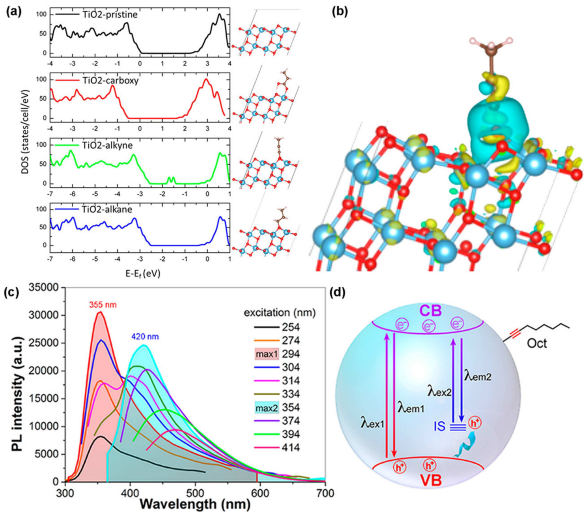

Figure 4. (a) Total density of states (TDOS) and interfacial configurations of a pristine TiO_2 slab (black curve) and slabs functionalized by carboxyl (-COOH, red curve), alkynyl (-C≡C-, green curve) and alkanyl (-CH_2-CH_2-, blue curve) ligands. (b) Bader charge transfer between alkynyl ligand and TiO_2 slab, where the cyan area indicates electron loss and yellow area indicates electron gain. The isosurface value is 0.003 e au^{-3}. (c) Photoluminescence spectra of TiO_2-HC8 at various excitation wavelengths. The shadowed ones represent maximal emissions at select excitation wavelengths. (d) Schematic illustration of the TiO_2-HC8 band structure based on the photoluminescence results. Reprinted with permission from ref.[106] © 2018 American Chemical Society.

band (VB) and conduction band (CB), which was denoted as the interfacial state (IS, ca. 0.5 eV above VB). Further calculations of the Bader charge (Figure 4b) showed that about 1.2 electrons were transferred to the TiO_2 slab per ligand. Experimentally, the photoluminescence emission (Figure 4c) of octyne-capped TiO_2 (TiO_2-HC8) nanoparticles indeed suggested the formation of a new interfacial state, with two emission peaks observed at ca. 355 nm and 420 nm under the excitation of 294 nm and 354 nm, respectively. The first one was contributed to bandedge emission, while the second one to CB-IS transition, consistent with results from DFT calculations. This is summarized in Figure 4d. That is, a new interfacial state is formed as the result of the interaction between the C≡CH anchor and TiO_2. This may be exploited for a deliberate manipulation of the nanoparticle optical and electronic properties and applications.

For instance, when a chromophore, such as ethynylpyrene (EPy), was bound onto TiO_2 via a –C≡CH anchor, a strong sensitization was observed.[106] UV-vis absorption measurements (Figure 5a) showed that the $S_0 \rightarrow S_n$ transition of the pyrene moiety in TiO_2-EPy red-shifted slightly, as compared to EPy monomers.[108–109] In addition, from Figure 5a inset, the effective bandgap of TiO_2-EPy was found to decrease to 2.94 eV, as compared to that of TiO_2-HC8 (3.51 eV), due to dominating electronic transitions via the IS. Consistent results were obtained by steady state photoluminescence (SSPL) measurements, as depicted in Figure 5b. Monomeric EPy exhibited several sharp peaks at around 382, 402 and 425 nm due to $S_0 \rightarrow S_n$ transitions when excited at 355 nm, while these peaks were diminished for TiO_2-EPy and a new peak centered at 420 nm emerged, which was the same as that of TiO_2-HC8. This indicates that the photoluminescence was due to the recombination of CB electrons and IS holes of TiO_2. Furthermore, the photoluminescence quantum yield (ϕ) was estimated to be about 36.6% for TiO_2-EPy, as compared to only 6.9% for TiO_2-HC8, indicating that the photoluminescence was sensitized due to charge donation from the pyrene group to TiO_2 CB. A schematic diagram of the charge transfer pathway was illustrated in Figure 5c. Besides SSPL, time-resolved photoluminescence (TRPL) was also carried out to study the charge transfer dynamics using a pulsed laser excitation at 337 nm. As shown in Figure 5d, EPy monomers showed a long lifetime of 16.52 ns, while the TiO_2-HC8 exhibited a markedly shorter lifetime of 1.18 ns. As for TiO_2-EPy, two lifetimes were identified at 1.66 ns (98.4%) and 9.76 ns (1.6%), which could be assigned to the fast decay via IS and the slow decay of pyrene, and the dominant pathway was the fast decay from TiO_2 CB to IS. This again confirmed the efficient charge donation from pyrene to TiO_2 CB, which is consistent with SSPL results. However, when pyrene was anchored on TiO_2 surface via –COOH, no obvious change was observed, compared to pyrene carboxylic acid monomers (PyCA), suggesting low-efficiency charge transfer via the –COOH anchor. This unique structure was successfully used as a dye (pyrene)-sensitized photocatalyst for the degradation of methylene blue (MB), where the degradation rate constant was about 4 times that of TiO_2-PyCA (Figure 5e–f).

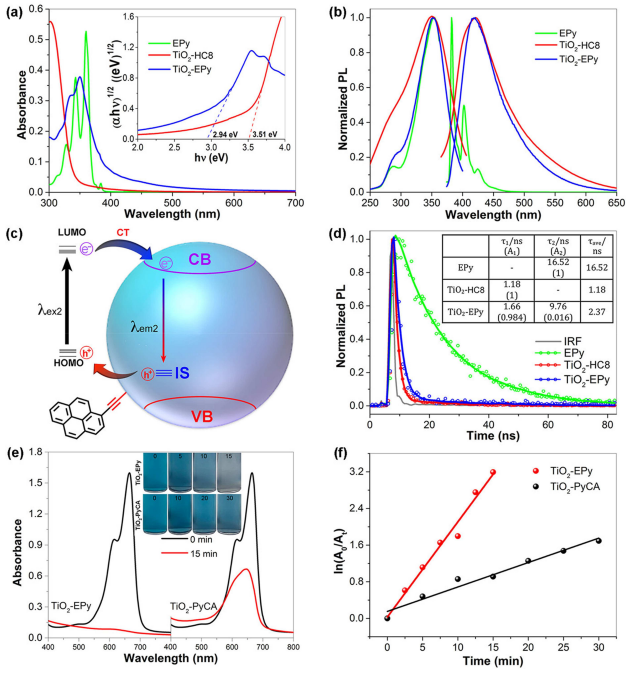

Figure 5. (a) UV−vis spectra of EPy monomers, TiO_2-EPy, and TiO_2-HC8. Inset shows the Tauc plots of TiO_2-EPy and TiO_2-HC8. (b) Normalized steady-state photoluminescence spectra of EPy monomers, TiO_2-EPy, and TiO_2-HC8. (c) Schematic diagram of charge transfer pathways at the TiO_2-EPy interface. (d) TRPL decay profiles of EPy monomers, TiO_2-EPy, and TiO_2-HC8. (e) UV−vis spectra of a methylene blue solution containing TiO_2-EPy or TiO_2-PyCA as photocatalysts before and after UV photoirradiation for 15 min. Insets are digital photographs of the solutions under UV photoirradiation for a different period of time (up to 30 min). (f) The corresponding degradation rate of methylene blue. Reprinted with permission from ref.[106] © 2018 American Chemical Society.

Similar effects of acetylene capping ligands on nanoparticle electronic properties are anticipated for oxides of other transition metals with the number of d electrons varied from 1 to 10, on the basis of DFT calculations.[106] This suggests that such interfacial engineering may seve as a generic, effective strategy in manipulating the materials properties and applications of metal oxide nanoparticles.

The electrochemical properties of TiO_2 nanoparticles can also be controlled by the nature of the interfacial bonds. In another study,[107] EFc was again used as the molecular probe and capping ligands for TiO_2 nanoparticles. The TiO_2-EFc (Figure 6a) nanoparticles were synthesized in the same manner,[106] and exhibited a bandgap of about 3.3 eV, as manifested in the Tauc plot in Figure 6b inset.[110] Consistent behaviors were observed in photoluminescence measurements

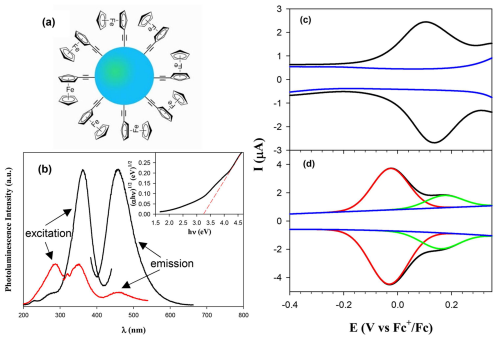

Figure 6. (a) Schematic structure of TiO_2-EFc nanoparticles. (b) Steady-state photoluminescence spectra of TiO_2-EFc nanoparticles in $CHCl_3$. Inset is the corresponding Tauc plot derived from the UV-vis absorption spectrum. SWVs of 2 mg mL^{-1} TiO_2-EFc nanoparticles recorded at a gold electrode with an increment of potential of 2 mV, amplitude of 25 mV and frequency 15 Hz (c) in the dark and (d) under 365 nm photoirradiation. Blue curves are background currents; black curves are experimental data, and red and green curves in (d) are deconvolution fits. Reprinted with permission from ref[107] © 2016 Elsevier Ltd.

(Figure 6b), where an emission peak can be identified at 351 nm (3.5 eV) under the excitation of 288 nm, due to the recombination of CB-VB. Interestingly, a second emission centered at 459 nm was observed when the nanoparticles were excited at 362 nm, which was most likely due to the recombination of CB-IS, as discussed earlier.[106] In addition, electrochemical measurements showed photo-induced IVCT. As shown in Figure 6c, a pair of voltammetric peaks can be observed in the dark at the formal potential of $E^{\circ\prime} = +122$ mV versus Fc^+/Fc, due to the redox reaction of the ferrocene moieties on TiO_2. However, under UV (365 nm) photoirradiation, two pairs of voltammetric peaks appeared with the formal potentials of −28 mV and +170 mV. This is consistent with the IVCT characteristics of a Class II compound.[111–112]

4. Summaries and Perspectives

In summary, breakthroughs from recent studies have shown that intraparticle charge transfer of semiconductor nanoparticles can be enhanced with conjugated core-ligand interfacial linkages, akin to the metal counterparts. This can be achieved by using olefin and acetylene derivatives as the capping ligands, where the reduced interfacial impedance facilitates electronic coupling between the organic ligands and nanoparticle cores. Such unique interfacial chemistry can be exploited as an effective addition to the tool box for nanoparticle surface functionalization and structural engineering, a critical step towards their diverse applications.

This raises an immediate, interesting question. Will the same chemistry be applicable to other semiconductor nanoparticles, such as metal chalcogenides, nitrides, and carbides? Note that these semiconductor nanoparticles have also found a wide range of applications, where a fundamental understanding of the mechanistic control of their optical and electronic properties plays an indispensable role.[113–114] Development of effective chemistries for the deliberate surface functionalization represents a key strategy.

Strategically, this involves rational design and engineering of both the point of anchor and the attached functional moiety. For the former, a great deal can be learned from advances in organometallic chemistry;[115] whereas the latter entails tailoring the chemical structure of the capping ligands for specific properties/applications, some of which are highlighted above. Notably, the ligand-core interfacial charge transfer may be further manipulated by the incorporation of electron-withdrawing/-donating moiety into the capping ligands. Apparent effects have been observed with metal nanoparticles.[116–118] An immediate question arises. How will such interfacial engineering impact the DOS and energy of the IS and hence the optical and electronic properties of semiconductor nanoparticles? These will be the focus of future studies.

Acknowledgements

This work was supported by the National Science Foundation (CHE-1710408 and CBET-1848841). Y. P. acknowledges the support of a Chancellor's Dissertation Year Fellowship of the University of California at Santa Cruz.

References

[1] W. J. Youngblood, S. H. A. Lee, Y. Kobayashi, E. A. Hernandez-Pagan, P. G. Hoertz, T. A. Moore, A. L. Moore, D. Gust, T. E. Mallouk, *J. Am. Chem. Soc.* **2009**, *131*, 926–927.
[2] A. Yella, H. W. Lee, H. N. Tsao, C. Y. Yi, A. K. Chandiran, M. K. Nazeeruddin, E. W. G. Diau, C. Y. Yeh, S. M. Zakeeruddin, M. Gratzel, *Science* **2011**, *334*, 629–634.
[3] B. A. Kairdolf, A. M. Smith, T. H. Stokes, M. D. Wang, A. N. Young, S. M. Nie, *Annu. Rev. Anal. Chem.* **2013**, *6*, 143–162.
[4] L. I. Berger, *Semiconductor materials*, CRC Press, Boca Raton, **1997**.
[5] B. G. Yacobi, *Semiconductor materials : an introduction to basic principles*, Kluwer Academic/Plenum Publishers, New York, **2003**.
[6] S. Silvi, A. Credi, *Chem. Soc. Rev.* **2015**, *44*, 4275–4289.
[7] H. Heinz, C. Pramanik, O. Heinz, Y. F. Ding, R. K. Mishra, D. Marchon, R. J. Flatt, I. Estrela-Lopis, J. Llop, S. Moya, R. F. Ziolo, *Surf. Sci. Rep.* **2017**, *72*, 1–58.

[8] M. C. Long, J. Brame, F. Qin, J. M. Bao, Q. L. Li, P. J. J. Alvarez, *Environ. Sci. Technol.* **2017**, *51*, 514–521.
[9] S. U. M. Khan, M. Al-Shahry, W. B. Ingler, *Science* **2002**, *297*, 2243–2245.
[10] B. Oregan, M. Gratzel, *Nature* **1991**, *353*, 737–740.
[11] J. B. Yang, P. Ganesan, J. Teuscher, T. Moehl, Y. J. Kim, C. Y. Yi, P. Comte, K. Pei, T. W. Holcombe, M. K. Nazeeruddin, J. L. Hua, S. M. Zakeeruddin, H. Tian, M. Gratzel, *J. Am. Chem. Soc.* **2014**, *136*, 5722–5730.
[12] L. Cao, X. Wang, M. J. Meziani, F. S. Lu, H. F. Wang, P. J. G. Luo, Y. Lin, B. A. Harruff, L. M. Veca, D. Murray, S. Y. Xie, Y. P. Sun, *J. Am. Chem. Soc.* **2007**, *129*, 11318.
[13] S. Ardo, G. J. Meyer, *Chem. Soc. Rev.* **2009**, *38*, 115–164.
[14] X. H. Gao, Y. Y. Cui, R. M. Levenson, L. W. K. Chung, S. M. Nie, *Nat. Biotechnol.* **2004**, *22*, 969–976.
[15] W. Z. Guo, J. J. Li, Y. A. Wang, X. G. Peng, *Chem. Mater.* **2003**, *15*, 3125–3133.
[16] N. C. Greenham, X. G. Peng, A. P. Alivisatos, *Phys. Rev. B* **1996**, *54*, 17628–17637.
[17] G. Zhang, G. Kim, W. Choi, *Energy Environ. Sci.* **2014**, *7*, 954–966.
[18] Y. M. Cho, H. Kyung, W. Choi, *Appl Catal B-Environ* **2004**, *52*, 23–32.
[19] N. Nakayama, T. Hayashi, *Colloids Surf. A* **2008**, *317*, 543–550.
[20] X. Zhang, X. K. Li, N. S. Deng, *Ind. Eng. Chem. Res.* **2012**, *51*, 704–709.
[21] Y. S. Seo, C. Lee, K. H. Lee, K. B. Yoon, *Angew. Chem. Int. Ed.* **2005**, *44*, 910–913; *Angew. Chem.* **2005**, *117*, 932–935.
[22] J. Zhao, T. Minegishi, L. Zhang, M. Zhong, Gunawan, M. Nakabayashi, G. J. Ma, T. Hisatomi, M. Katayama, S. Ikeda, N. Shibata, T. Yamada, K. Domen, *Angew. Chem. Int. Ed.* **2014**, *53*, 11808–11812; *Angew. Chem.* **2014**, *126*, 12002–12006.
[23] J. A. Dean, *Large's Handbook of Chemistry*, 15th ed., McGraw-Hill, Inc., New York, **1999**.
[24] P. G. Hu, L. M. Chen, X. W. Kang, S. W. Chen, *Acc. Chem. Res.* **2016**, *49*, 2251–2260.
[25] E. C. Cho, S. Park, X. J. Hao, D. Y. Song, G. Conibeer, S. C. Park, M. A. Green, *Nanotechnology* **2008**, *19*, 245201.
[26] N. M. Park, T. S. Kim, S. J. Park, *Appl. Phys. Lett.* **2001**, *78*, 2575–2577.
[27] R. Ban, F. F. Zheng, J. R. Zhang, *Anal. Methods* **2015**, *7*, 1732–1737.
[28] Z. H. Kang, C. H. A. Tsang, N. B. Wong, Z. D. Zhang, S. T. Lee, *J. Am. Chem. Soc.* **2007**, *129*, 12090–12091.
[29] F. Priolo, T. Gregorkiewicz, M. Galli, T. F. Krauss, *Nat. Nanotechnol.* **2014**, *9*, 19–32.
[30] J. M. Buriak, M. J. Allen, *J. Am. Chem. Soc.* **1998**, *120*, 1339–1340.
[31] J. M. Buriak, M. P. Stewart, T. W. Geders, M. J. Allen, H. C. Choi, J. Smith, D. Raftery, L. T. Canham, *J. Am. Chem. Soc.* **1999**, *121*, 11491–11502.
[32] T. K. Purkait, M. Iqbal, M. H. Wahl, K. Gottschling, C. M. Gonzalez, M. A. Islam, J. G. Veinot, *J. Am. Chem. Soc.* **2014**, *136*, 17914–17917.
[33] M. A. Islam, T. K. Purkait, M. H. Mobarok, I. M. D. Hoehlein, R. Sinelnikov, M. Iqbal, D. Azulay, I. Balberg, O. Millo, B. Rieger, J. G. C. Veinot, *Angew. Chem. Int. Ed.* **2016**, *55*, 7393–7397; *Angew. Chem.* **2016**, *128*, 7519–7523.
[34] J. A. Kelly, J. G. C. Veinot, *ACS Nano* **2010**, *4*, 4645–4656.
[35] M. Dasog, J. Kehrle, B. Rieger, J. G. C. Veinot, *Angew. Chem. Int. Ed.* **2016**, *55*, 2322–2339; *Angew. Chem.* **2016**, *128*, 2366–2384.
[36] A. Gupta, M. T. Swihart, H. Wiggers, *Adv. Funct. Mater.* **2009**, *19*, 696–703.
[37] C. S. Yang, R. A. Bley, S. M. Kauzlarich, H. W. H. Lee, G. R. Delgado, *J. Am. Chem. Soc.* **1999**, *121*, 5191–5195.
[38] F. J. Hua, M. T. Swihart, E. Ruckenstein, *Langmuir* **2005**, *21*, 6054–6062.
[39] M. Rosso-Vasic, E. Spruijt, B. van Lagen, L. De Cola, H. Zuilhof, *Small* **2008**, *4*, 1835–1841.
[40] S. P. Ashby, J. A. Thomas, J. Garcia-Canadas, G. Min, J. Corps, A. V. Powell, H. L. Xu, W. Shen, Y. M. Chao, *Faraday Discuss.* **2014**, *176*, 349–361.
[41] B. Sweryda-Krawiec, T. Cassagneau, J. H. Fendler, *J. Phys. Chem. B* **1999**, *103*, 9524–9529.
[42] Q. Li, T. Y. Luo, M. Zhou, H. Abroshan, J. C. Huang, H. J. Kim, N. L. Rosi, Z. Z. Shao, R. C. Jin, *ACS Nano* **2016**, *10*, 8385–8393.
[43] E. Rogozhina, G. Belomoin, A. Smith, L. Abuhassan, N. Barry, O. Akcakir, P. V. Braun, M. H. Nayfeh, *Appl. Phys. Lett.* **2001**, *78*, 3711–3713.
[44] M. Dasog, K. Bader, J. G. C. Veinot, *Chem. Mater.* **2015**, *27*, 1153–1156.
[45] R. K. Baldwin, K. A. Pettigrew, J. C. Garno, P. P. Power, G. Y. Liu, S. M. Kauzlarich, *J. Am. Chem. Soc.* **2002**, *124*, 1150–1151.
[46] R. D. Tilley, J. H. Warner, K. Yamamoto, I. Matsui, H. Fujimori, *Chem. Commun.* **2005**, 1833–1835.
[47] F. A. Reboredo, G. Galli, *J. Phys. Chem. B* **2005**, *109*, 1072–1078.
[48] A. Gali, M. Voros, D. Rocca, G. T. Zimanyi, G. Galli, *Nano Lett.* **2009**, *9*, 3780–3785.
[49] H. S. Li, Z. G. Wu, T. L. Zhou, A. Sellinger, M. T. Lusk, *Phys. Chem. Chem. Phys.* **2014**, *16*, 19275–19281.
[50] T. L. Zhou, R. T. Anderson, H. S. Li, J. Bell, Y. A. Yang, B. P. Gorman, S. Pylypenko, M. T. Lusk, A. Sellinger, *Nano Lett.* **2015**, *15*, 3657–3663.
[51] Y. Peng, C. P. Deming, S. W. Chen, *ChemElectroChem* **2016**, *3*, 1219–1224.
[52] P. G. Hu, L. M. Chen, J. E. Lu, H. W. Lee, S. W. Chen, *Langmuir* **2018**, *34*, 2834–2840.
[53] L. M. Chen, P. G. Hu, C. P. Deming, W. Li, L. G. Li, S. W. Chen, *J. Phys. Chem. C* **2015**, *119*, 15449–15454.
[54] L. M. Chen, Y. Song, P. G. Hu, C. P. Deming, Y. Guo, S. W. Chen, *Phys. Chem. Chem. Phys.* **2014**, *16*, 18736–18742.
[55] X. W. Kang, N. B. Zuckerman, J. P. Konopelski, S. W. Chen, *J. Am. Chem. Soc.* **2012**, *134*, 1412–1415.
[56] S. Deb-Choudhury, S. Prabakar, G. Krsinic, J. M. Dyer, R. D. Tilley, *J. Agric. Food Chem.* **2013**, *61*, 7188–7194.
[57] J. Liu, C. H. Liang, Z. F. Tian, S. Y. Zhang, G. S. Shao, *Sci. Rep.* **2013**, *3*, 1741.

[58] E. Muthuswamy, A. S. Iskandar, M. M. Amador, S. M. Kauzlarich, *Chem. Mater.* **2013**, *25*, 1416–1422.
[59] T. K. Purkait, A. K. Swarnakar, G. B. De Los Reyes, F. A. Hegmann, E. Rivard, J. G. C. Veinot, *Nanoscale* **2015**, *7*, 2241–2244.
[60] M. I. Asghar, K. Miettunen, J. Halme, P. Vahermaa, M. Toivola, K. Aitola, P. Lund, *Energy Environ. Sci.* **2010**, *3*, 418–426.
[61] A. Hagfeldt, G. Boschloo, L. C. Sun, L. Kloo, H. Pettersson, *Chem. Rev.* **2010**, *110*, 6595–6663.
[62] P. T. Nguyen, A. R. Andersen, E. M. Skou, T. Lund, *Sol. Energy Mater. Sol. Cells* **2010**, *94*, 1582–1590.
[63] K. Sodeyama, M. Sumita, C. O'Rourke, U. Terranova, A. Islam, L. Han, D. R. Bowler, Y. Tateyama, *J. Phys. Chem. Lett.* **2012**, *3*, 472–477.
[64] D. L. Ashford, W. Song, J. J. Concepcion, C. R. Glasson, M. K. Brennaman, M. R. Norris, Z. Fang, J. L. Templeton, T. J. Meyer, *J. Am. Chem. Soc.* **2012**, *134*, 19189–19198.
[65] K. Hu, K. C. D. Robson, P. G. Johansson, C. P. Berlinguette, G. J. Meyer, *J. Am. Chem. Soc.* **2012**, *134*, 8352–8355.
[66] H. Y. Chen, S. Ardo, *Nat. Chem.* **2018**, *10*, 17–23.
[67] S. Ye, A. Kathiravan, H. Hayashi, Y. J. Tong, Y. Infahsaeng, P. Chabera, T. Pascher, A. P. Yartsev, S. Isoda, H. Imahori, V. Sundstrom, *J. Phys. Chem. C* **2013**, *117*, 6066–6080.
[68] R. Long, D. Casanova, W. H. Fang, O. V. Prezhdo, *J Am Soc Chem* **2017**, *139*, 2619–2629.
[69] B. Fritzinger, R. K. Capek, K. Lambert, J. C. Martins, Z. Hens, *J. Am. Chem. Soc.* **2010**, *132*, 10195–10201.
[70] S. M. Harrell, J. R. McBride, S. J. Rosenthal, *Chem. Mater.* **2013**, *25*, 1199–1210.
[71] Z. Y. Huang, Z. H. Xu, M. Mahboub, X. Li, J. W. Taylor, W. H. Harman, T. Q. Lian, M. L. Tang, *Angew. Chem. Int. Ed.* **2017**, *56*, 16583–16587; *Angew. Chem.* **2017**, *129*, 16810–16814.
[72] X. Li, V. M. Nichols, D. P. Zhou, C. Lim, G. S. H. Pau, C. J. Bardeen, M. L. Tang, *Nano Lett.* **2014**, *14*, 3382–3387.
[73] L. R. Hou, Q. Zhang, L. T. Ling, C. X. Li, L. Chen, S. Chen, *J. Am. Chem. Soc.* **2013**, *135*, 10618–10621.
[74] D. Zherebetskyy, M. Scheele, Y. J. Zhang, N. Bronstein, C. Thompson, D. Britt, M. Salmeron, P. Alivisatos, L. W. Wang, *Science* **2014**, *344*, 1380–1384.
[75] M. Puri, V. E. Ferry, *ACS Nano* **2017**, *11*, 12240–12246.
[76] E. Galoppini, *Coord. Chem. Rev.* **2004**, *248*, 1283–1297.
[77] S. Altobello, C. A. Bignozzi, S. Caramori, G. Larramona, S. Quici, G. Marzanni, R. Lakhmiri, *J. Photochem. Photobiol. A* **2004**, *166*, 91–98.
[78] B. J. Brennan, M. J. L. Portoles, P. A. Liddell, T. A. Moore, A. L. Moore, D. Gust, *Phys. Chem. Chem. Phys.* **2013**, *15*, 16605–16614.
[79] T. P. Brewster, S. J. Konezny, S. W. Sheehan, L. A. Martini, C. A. Schmuttenmaer, V. S. Batista, R. H. Crabtree, *Inorg. Chem.* **2013**, *52*, 6752–6764.
[80] C. Koenigsmann, T. S. Ripollese, B. J. Brennan, C. F. A. Negre, M. Koepf, A. C. Durrell, R. L. Milot, J. A. Torre, R. H. Crabtree, V. S. Batista, G. W. Brudvig, J. Bisquert, C. A. Schmuttenmaer, *Phys. Chem. Chem. Phys.* **2014**, *16*, 16629–16641.
[81] W. R. McNamara, R. L. Milot, H. E. Song, R. C. Snoeberger, V. S. Batista, C. A. Schmuttenmaer, G. W. Brudvig, R. H. Crabtree, *Energy Environ. Sci.* **2010**, *3*, 917–923.
[82] H. Park, E. Bae, J. J. Lee, J. Park, W. Choi, *J. Phys. Chem. B* **2006**, *110*, 8740–8749.
[83] J. N. Clifford, E. Martinez-Ferrero, A. Viterisi, E. Palomares, *Chem. Soc. Rev.* **2011**, *40*, 1635–1646.
[84] R. L. Milot, C. A. Schmuttenmaer, *Acc. Chem. Res.* **2015**, *48*, 1423–1431.
[85] N. C. Anderson, M. P. Hendricks, J. J. Choi, J. S. Owen, *J. Am. Chem. Soc.* **2013**, *135*, 18536–18548.
[86] R. Gomes, A. Hassinen, A. Szczygiel, Q. A. Zhao, A. Vantomme, J. C. Martins, Z. Hens, *J. Phys. Chem. Lett.* **2011**, *2*, 145–152.
[87] I. Lopez-Duarte, M. K. Wang, R. Humphry-Baker, M. Ince, M. V. Martinez-Diaz, M. K. Nazeeruddin, T. Torres, M. Gratzel, *Angew. Chem. Int. Ed.* **2012**, *51*, 1895–1898; *Angew. Chem.* **2012**, *124*, 1931–1934.
[88] D. F. Zigler, Z. A. Morseth, L. Wang, D. L. Ashford, M. K. Brennaman, E. M. Grumstrup, E. C. Brigham, M. K. Gish, R. J. Dillon, L. Alibabaei, G. J. Meyer, T. J. Meyer, J. M. Papanikolas, *J. Am. Chem. Soc.* **2016**, *138*, 4426–4438.
[89] F. Chen, W. W. Zou, W. W. Qu, J. L. Zhang, *Catal. Commun.* **2009**, *10*, 1510–1513.
[90] D. Jiang, Y. Xu, D. Wu, Y. H. Sun, *Appl Catal B-Environ* **2009**, *88*, 165–172.
[91] Y. Ooyama, S. Inoue, T. Nagano, K. Kushimoto, J. Ohshita, I. Imae, K. Komaguchi, Y. Harima, *Angew. Chem. Int. Ed.* **2011**, *50*, 7429–7433; *Angew. Chem.* **2011**, *123*, 7567–7571.
[92] Y. Ooyama, N. Yamaguchi, I. Imae, K. Komaguchi, J. Ohshita, Y. Harima, *Chem. Commun.* **2013**, *49*, 2548–2550.
[93] X. Q. Meng, A. Pant, H. Cai, J. Kang, H. Sahin, B. Chen, K. D. Wu, S. J. Yang, A. Suslu, F. M. Peeters, S. Tongay, *Nanoscale* **2015**, *7*, 17109–17115.
[94] J. Massin, L. Ducasse, T. Toupance, C. Olivier, *J. Phys. Chem. C* **2014**, *118*, 10677–10685.
[95] W. R. McNamara, R. C. Snoeberger, G. Li, J. M. Schleicher, C. W. Cady, M. Poyatos, C. A. Schmuttenmaer, R. H. Crabtree, G. W. Brudvig, V. S. Batista, *J. Am. Chem. Soc.* **2008**, *130*, 14329–14338.
[96] T. Kamegawa, S. Matsuura, H. Seto, H. Yamashita, *Angew. Chem. Int. Ed.* **2013**, *52*, 916–919; *Angew. Chem.* **2013**, *125*, 950–953.
[97] E. Amstad, T. Gillich, I. Bilecka, M. Textor, E. Reimhult, *Nano Lett.* **2009**, *9*, 4042–4048.
[98] T. Rajh, L. X. Chen, K. Lukas, T. Liu, M. C. Thurnauer, D. M. Tiede, *J. Phys. Chem. B* **2002**, *106*, 10543–10552.
[99] T. Lana-Villarreal, A. Rodes, J. M. Perez, R. Gomez, *J. Am. Chem. Soc.* **2005**, *127*, 12601–12611.
[100] J. M. Notestein, E. Iglesia, A. Katz, *Chem. Mater.* **2007**, *19*, 4998–5005.
[101] Y. Park, N. J. Singh, K. S. Kim, T. Tachikawa, T. Majima, W. Choi, *Chem. Eur. J.* **2009**, *15*, 10843–10850.
[102] C. J. Xu, K. M. Xu, H. W. Gu, R. K. Zheng, H. Liu, X. X. Zhang, Z. H. Guo, B. Xu, *J. Am. Chem. Soc.* **2004**, *126*, 9938–9939.

[103] R. Marczak, F. Werner, J. F. Gnichwitz, A. Hirsch, D. M. Guldi, W. Peukert, *J. Phys. Chem. C* **2009**, *113*, 4669–4678.
[104] H. F. Wang, Y. Y. Wu, X. P. Yan, *Anal. Chem.* **2013**, *85*, 1920–1925.
[105] W. Lin, J. Walter, A. Burger, H. Maid, A. Hirsch, W. Peukert, D. Segets, *Chem. Mater.* **2015**, *27*, 358–369.
[106] Y. Peng, B. Lu, F. Wu, F. Zhang, J.-E. Lu, X. Kang, Y. Ping, S. Chen, *J. Am. Chem. Soc.* **2018**, *140*, 15290–15299.
[107] Y. Peng, J. E. Lu, C. P. Deming, L. M. Chen, N. Wang, E. Y. Hirata, S. W. Chen, *Electrochim. Acta* **2016**, *211*, 704–710.
[108] X. G. Li, Y. W. Liu, M. R. Huang, S. Peng, L. Z. Gong, M. G. Moloney, *Chem. Eur. J.* **2010**, *16*, 4803–4813.
[109] M. Amelia, A. Lavie-Cambot, N. D. McClenaghan, A. Credi, *Chem. Commun.* **2011**, *47*, 325–327.
[110] K. M. Reddy, S. V. Manorama, A. R. Reddy, *Mater. Chem. Phys.* **2003**, *78*, 239–245.
[111] S. F. Nelsen, *Chem. Eur. J.* **2000**, *6*, 581–588.
[112] M. B. Bobin, P. Day, *Adv. Inorg. Chem. Radiochem.* **1968**, *10*, 247–422.
[113] A. Fernando, K. L. Dimuthu, M. Weerawardene, N. V. Karimova, C. M. Aikens, *Chem. Rev.* **2015**, *115*, 6112–6216.
[114] J. R. Xiao, S. H. Yang, F. Feng, H. G. Xue, S. P. Guo, *Coord. Chem. Rev.* **2017**, *347*, 23–47.
[115] R. J. Ouellette, J. D. Rawn, *Organic chemistry : structure, mechanism, synthesis*, Second edition, Academic Press, London; San Diego, CA, **2018**.
[116] Z. Y. Zhou, X. W. Kang, Y. Song, S. W. Chen, *J. Phys. Chem. C* **2012**, *116*, 10592–10598.
[117] Z. Y. Zhou, X. W. Kang, Y. Song, S. W. Chen, *Chem. Commun.* **2012**, *48*, 3391–3393.
[118] P. G. Hu, L. M. Chen, C. P. Deming, J. E. Lu, L. W. Bonny, S. W. Chen, *Nanoscale* **2016**, *8*, 12013–12021.

Manuscript received: February 21, 2019
Revised manuscript received: April 17, 2019
Version of record online: May 7, 2019

